JOURNAL OF CHEMICAL INFORMATION AND MODELING

Article

pubs.acs.org/jcim

# Making Sense of Large-Scale Kinase Inhibitor Bioactivity Data Sets: A Comparative and Integrative Analysis

Jing Tang,* Agnieszka Szwajda, Sushil Shakyawar, Tao Xu, Petteri Hintsanen, Krister Wennerberg, and Tero Aittokallio

Institute for Molecular Medicine Finland (FIMM), University of Helsinki, Tukholmankatu 8, FI-00290, Helsinki, Finland

Supporting Information

**ABSTRACT:** We carried out a systematic evaluation of target selectivity profiles across three recent large-scale biochemical assays of kinase inhibitors and further compared these standardized bioactivity assays with data reported in the widely used databases ChEMBL and STITCH. Our comparative evaluation revealed relative benefits and potential limitations among the bioactivity types, as well as pinpointed biases in the database curation processes. Ignoring such issues in data heterogeneity and representation may lead to biased modeling of drugs' polypharmacological effects as well as to unrealistic evaluation of computational strategies for the prediction of drug–target interaction networks. Toward making use of the complementary information captured by the various bioactivity types, including $IC_{50}$, $K_i$, and $K_d$, we also introduce a model-based integration approach, termed KIBA, and demonstrate here how it can be used to classify kinase inhibitor targets and to pinpoint potential errors in database-reported drug–target interactions. An integrated drug–target bioactivity matrix across 52 498 chemical compounds and 467 kinase targets, including a total of 246 088 KIBA scores, has been made freely available.

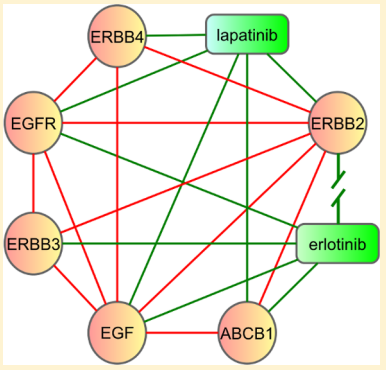


## INTRODUCTION

Many drug molecules elicit their bioactivities by modulating multiple cellular targets.[1,2] Improved understanding and prediction of such polypharmacological effects is critical for the development of more effective and less toxic drug treatments either by multitarget drugs or targeted drug combinations.[3,4] Multitarget treatments are being considered as a promising strategy to tackle the compensatory mechanisms and robustness of cellular systems, especially in anticancer drug developments, where the possibility to selectively inhibit cancer-cell-specific panels of cellular targets provides an unprecedented potential for improved therapeutic potency and reduced resistance and side effects.[5−7] However, the efficacy and toxicity of chemical compounds is often a result of a complex interplay between signaling pathways on the biological systems, initiated by the promiscuous drug–target interactions and then propagated throughout the whole cellular networks.[4,8] In particular, the observed drug response is not only based on the intended primary targets, which produce the "on-target" therapeutic effect, but also on unintended secondary targets, which are responsible for the unwanted "off-target" effects that may either cause adverse events or contribute to the therapeutic effect. Therefore, systematic profiling of molecular targets provides important insights into the mechanisms of both therapeutic properties and side effects of the candidate drug compounds under investigation.[9]

Toward modeling and predicting polypharmacological effects of drugs, network models have recently gained much popularity in exploring the system-level mechanism behind drug action, resistance, and potential side-effects by connecting chemical compounds and their on and off targets in the context of biological networks and interconnected pathways.[2,10,11] Once carefully formulated in realistic research settings, these network models may facilitate more efficient and more context-specific drug development and testing pipelines in the future, with applications, for instance, toward improved drug repositioning or personalized medicine strategies.[12] Conventionally, system-level drug–target interactions are represented using relatively simplistic network models in which a compound and a protein has a binary on–off relation, such as interaction or no interaction.[13−17] While these studies have provided useful information on the topological properties of the global drug–target networks, such binary network models ignore many important aspects of the drug–target interactions, including their dose-dependence patterns and quantitative bioactivity readouts. Moreover, most of these studies tend to be focused on highly selected therapeutic areas, with potential biases toward clinically approved drugs and their known primary targets.[18]

To improve the coverage of the binary drug–target interaction networks for the discovery of new potential targets or off-target relationships at a proteome-wide level, there exist a number of public databases, including KEGG BRITE/DRUG,[19] BRENDA,[20] SuperTarget,[21] TTD,[22] and DrugBank,[23] which catalogue the observed or predicted cellular effects of chemicals

Received: December 1, 2013
Published: February 12, 2014

across various families of chemical compounds. While useful for many applications, a limitation of these databases is that the reported drug targets may originate from various types of evidence, such as those based on direct binding events or from downstream treatment effects, in addition to pharmacodynamic or pharmacogenomic investigation of protein−chemical associations, or even from computational predictions using, for instance, text mining algorithms. This results in highly heterogeneous sets of potential drug−target interactions, and the user is provided with only limited capabilities of evaluating how meaningful the interaction might be for a given application use case. Furthermore, these databases focus on the positive drug−target interactions, while the information about the negative cases is ignored, meaning that drug−target interactions that have been shown to be inactive are not tracked. Many statistical and machine learning models for inferring drug−target interaction networks validate their predictions using such *unary* data by assuming those unreported drug−target interactions as negative cases.[24,25] Ignoring the fundamental differences between *unreported* and *negative* drug−target interactions may dramatically affect both the sensitivity and specificity of the prediction models.[26,27]

ChEMBL is one of the major databases to collect and manage chemical and target annotations for a large number of bioactive drug-like small molecules.[28] These data are manually extracted from primary medicinal chemistry sources and further curated and standardized across a diverse set of target families. ChEMBL includes also compound bioactivity data derived from biochemical assays, which provide a quantitative means to characterize the full spectrum of interactions between the chemical compounds and their potential target space. Since ChEMBL includes quantitative bioactivity data, and therefore allows the user to define both positive and negative interactions, it has increasingly been used in many applications, including validation of computational predictions of drug targets[29−31] and understanding of the ligand-binding specificity at a system level.[32] However, despite its continuous efforts to increase the data coverage and accuracy, a major challenge for utilizing ChEMBL and other similar public resources is the proper treatment of data heterogeneity, as the collected bioactivity measurements often originate from various experimental settings. For instance, assessing a given drug−target interaction in ChEMBL often leads to multiple, largely incomparable assay readouts. Without going to the assay details, it is difficult to evaluate the measurement reliability behind the various bioactivity values.[33,34]

In the present study, we first carried out a comparative evaluation of the target selectivity profiles as extracted from three recent large-scale biochemical assays of kinase inhibitors.[35−37] These systematic experimental mappings provide highly specific drug−target interaction profiles, either in terms of thermodynamic dissociation constants ($K_d$ or $K_i$) or remaining enzyme activity (Activity %), measured with standardized assays under controlled experimental settings. We focused here on the kinase target family because of its essential roles in cellular signaling transduction for many cancers and inflammatory diseases. Assessing the experimental uncertainty between the independent bioactivity assays enables a systematic characterization of the kinase target spectrum of both on- and off-target interactions, which is of primary importance for understanding the polypharmacological effects of kinase inhibitors. The reported drug−target interactions were further compared with the quantitative data from ChEMBL and unary interactions from an integrated database resource, STITCH, which links chemicals and proteins by evidence derived from experimental assays as well as from text mining the literature and several other databases.[38] We further introduced a method, Kinase Inhibitor BioActivity (KIBA), which integrates the information from $IC_{50}$, $K_i$, and $K_d$ measurements into a single bioactivity score toward improved drug−target interaction classification. By means of the KIBA integration, we compiled a bioactivity matrix across 52 498 kinase inhibitors and 467 human kinases, from which the positive and negative ends of the drug−target interactions can be inferred.

## MATERIALS AND METHODS

**Comparison of the Three Kinase Inhibitor Studies.** We used the quantitative data from three large-scale biochemical studies of bioactivity profiling of small-molecule protein kinase inhibitors. The Davis study[35] utilized ATP site-dependent competition binding assays for a total of 72 compounds tested against 442 kinase proteins and measured the dissociation constant ($K_d$) for each drug−target pair. The Metz study[36] applied a more conventional kinase activity assay measuring the inhibition constant ($K_i$) of the transfer of a radioactive phosphate group to target peptides for a larger compound collection, including 1493 structures that have been deposited to PubChem and tested against a smaller panel including 172 protein kinases. The Anastassiadis study[37] directly measured the remaining catalytic activities for 300 kinases toward 178 kinase inhibitors tested at a single concentration of 0.5 $\mu$M and reported the activity percentages as a readout.

To enable cross-comparison, the drug−target interactions reported in the three studies were mapped into ChEMBL and STITCH using their corresponding ChEMBL IDs and UniProt IDs. Missing values reported in the Davis study were input with 10 000 nM as these drug−target pairs were tested but for which the binding was either weak ($K_d$ > 10 000 nM) or not detected in the primary screen at the maximal concentration (10 000 nM). Missing values in the Metz and Anastassiadis studies, however, represent nonmeasured drug−target interactions and thus were simply excluded from the analysis. We focused on catalytically active human protein kinases and therefore removed noncatalytic kinases and kinases from human pathogens. For the kinases that contain also mutant types in the Davis study, the minimal bioactivity value was recorded (see Supporting Information Table 1 for the list of mutated kinases). After such a preprocessing, there were $K_d$ values for 72 compounds and 379 kinases, $K_i$ values for 201 compounds and 169 kinases, and Activity percentage values for 145 compounds and 261 kinases. The pairwise overlaps of the compounds, targets, and drug−target interactions between the three studies are shown in Figure 1 and Table 1.

The three data sets were also compared with the bioactivity data of the same types that have been reported in other studies as extracted from the ChEMBL database (version 17). We restricted our analyses on the high-confidence biochemical assays for human targets (organism: "*Homo sapiens*" and confidence level ≥ 8, ensuring that there was a reported direct interaction between the ligand and protein target). For a drug−target interaction with multiple measurements, the median value was taken after excluding apparent outliers. Identical values due to duplication were removed. The studies from the same research groups or companies were excluded to avoid possible technical biases and repeated measurements. For


dx.doi.org/10.1021/ci400709d | J. Chem. Inf. Model. 2014, 54, 735−743

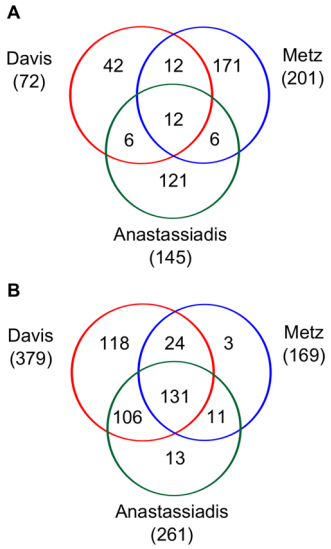


**Figure 1.** Overlap between the Davis $K_d$, Metz $K_i$, and Anastassiadis Activity data sets. (A) Common compounds. (B) Common targets. Only the compounds with ChEMBL IDs were considered in the comparative analysis. The numbers of overlapping drug–target interactions profiled in these data sets are provided in Table 1.

**Table 1. Pairwise Overlaps in Drug–Target Interactions between the Three Studies**[a]

| | Davis[35] | Metz[36] | Anastassiadis[37] |
|---|---|---|---|
| Davis | 27 288 | 2575 | 4255 |
| Metz | 14.33% | 17 966 | 2117 |
| Anastassiadis | 15.59% | 11.78% | 37 463 |

[a]Diagonal: the total number of compound–protein interactions that were measured in each of the three studies. Upper-diagonal: the pairwise overlaps between the three studies. Lower-diagonal: the percentages of the pairwise overlaps relative to the smaller study.

example, when querying ChEMBL $K_d$ values for the drug–target interactions that are reported in the Davis data, we removed the data from an earlier study by the same group which included a subset of the compounds.[38] Similarly, for the evaluation of the Metz $K_i$ data, we removed the multiple smaller-scale studies done in the Abbott Laboratories, which is the major affiliation of the Metz study (see Supporting Information Table 2 for the list of studies that were removed from the ChEMBL data).

Positive drug–target interactions were extracted from two sources. First, a list of 134 drug–target interactions was obtained from the Supplementary Table 3 of the Davis study, where it was shown that these drug–target interactions have been experimentally validated in multiple studies (referred to as PRIMARY interactions). A secondary list of positive drug–target interactions was derived from the STITCH database (version 3.0) by selecting only those interactions with combined confidence scores higher than 900. We utilized all the interaction types in STITCH in order to collect a representative and large enough set of positive drug–target interactions reported in the integrated knowledge databases (referred to as the STITCH interactions). These two lists of positive drug–target interactions were considered as the reference data for evaluating the reliability of the quantitative values from the three studies. However, we also pinpointed a number of drug–target interactions in the PRIMARY or STITCH list that might be false positives in light of the experimental data.

**Statistical Analyses.** The goodness of fit between the experimental data and positive drug–target interactions was evaluated using enrichment analysis. A high enrichment score (ES or NES for its normalized version) indicates lower than average bioactivity values for these drug–target interactions, and thus indicates a better fit. The enrichment scores were calculated on the basis of the Kolmogorov–Smirnov statistic in the GSEA (Gene Set Enrichment Analysis) tool.[40] For determination of the empirical bioactivity threshold for positive drug–target interactions, a hypergeometric test was used. The consistency between the bioactivity measurements was assessed using the Kendall correlation coefficient due to its robustness on non-normally distributed data and lower sensitivity to outliers and ties. For comparing the distributions of bioactivity values between the three studies and ChEMBL data, the two-sample Kolmogorov–Smirnov test was applied where a lower significance level (i.e., a higher p-value) indicates a better goodness-of-fit. Discrimination accuracy between true positive and negative interactions was assessed using area under the receiver operating characteristic curve (AUC). The significance of the observed difference between two AUCs was evaluated using the De Long test.[41] All of the statistical tests, if not mentioned specifically, were calculated using the statistical analysis program R.

**Distance Measures.** To evaluate the consistency between bioactivity types, we used two metrics. The Kendall correlation between two bioactivity types (say X and Y) is a function of rank orders between a pair of observations $(x_i, y_i)$ and $(x_j, y_j)$:

$$\tau = \frac{(a-b)}{n(n-1)/2} \quad (1)$$

where $a$ and $b$ stand for the number of concordant pairs and discordant pairs, defined as $a = |\{(i,j)\}|x_i < x_j$ and $y_i < y_j\}|$ and $b = |\{(i,j)\}|x_i < x_j$ and $y_i > y_j\}|$, respectively. An alternative distance metric is the Jaccard distance, which sums over the absolute deviations of the observed bioactivity values:

$$d = \frac{2\sum|y_i - x_i|}{\sum|x_i + y_i| + \sum|y_i - x_i|} \quad (2)$$

Jaccard distance takes values in the range of [0 1], with a higher value indicating more discrepancy between the bioactivity types.

**Integration of the Bioactivity Types.** In a typical enzymatic inhibition assay, $IC_{50}$, the concentration at which the inhibitor causes a 50% inhibition of enzymatic activity can be related to the inhibitor constant ($K_i$) using the Cheng-Prusoff model:[42]

$$K_i = \frac{IC_{50}}{1 + [S]/K_m} \quad (3)$$

Here, $[S]$ is the experimental substrate concentration and $K_m$ is the concentration of the substrate (e.g., ATP for ATP-competitive kinase inhibitors) at which enzyme activity is at half maximal. Since $[S]$ and $K_m$ vary in different protein–ligand systems, a direct transfer between $IC_{50}$ and $K_i$ is possible only if such information is available. Unfortunately, for most of the kinase inhibitor assays curated in ChEMBL, the information about experimental conditions is missing. However, recent efforts to explore the variability and reproducibility of ChEMBL


dx.doi.org/10.1021/ci400709d | J. Chem. Inf. Model. 2014, 54, 735–743

data have observed that the consistency within and between $IC_{50}$ and $K_i$ values is preserved at a sufficiently high level.[32−34] Despite the different constructs or different phosphorylation levels that might have been used in the bioactivity studies, one reason for such high consistency may be that traditional enzymatic inhibitor assays often are performed with the substrate at as low concentrations as possible, preferably well below the $K_m$, making the $IC_{50}$ and $K_i$ relatively similar, although this cannot be assumed to be the case in every assay. However, based on the strong correlation between $IC_{50}$ and $K_i$ values we and others have found throughout ChEMBL, we hypothesized that the functional relationship between $IC_{50}$ and $K_i$ bioactivity types (eq 3) would enable their integrative analysis for kinase inhibitors.

For a kinase inhibitor drug−target interaction, we consider the medians of three major bioactivity types ($IC_{50}$, $K_i$, and $K_d$) and then adjust the $K_i$ and $K_d$ using the parametric model:

$$K_i.\ \mathrm{adj} = \frac{IC_{50}}{1 + L_i(IC_{50}/K_i)}$$

$$K_d.\ \mathrm{adj} = \frac{IC_{50}}{1 + L_d(IC_{50}/K_d)} \quad (4)$$

where $L_i$ and $L_d$ are the parameters that determine the weights of $IC_{50}$ in the model-based adjustments for $K_i$ and $K_d$. The purpose of such functional adjustments is to utilize the information in $IC_{50}$ to maximize the consistency between $K_i$ and $K_d$. We allow the parameters $L_i$ and $L_d$ to be changed, so that the best adjustment can be achieved when the consistency between $K_i$ and $K_d$ is maximized. Utilizing a sequential sampling, we determined the optimal values for $L_i$ and $L_d$ and then adjusted $K_i$ and $K_d$ according to eq 4. The kinase inhibitor bioactivity (KIBA) score was defined as $K_i$.adj or $K_d$.adj, or the average of them, depending on the availability of the bioactivity types:

$$\mathrm{KIBA} = \begin{cases} K_i.\ \mathrm{adj} & \text{if } IC_{50} \text{ and } K_i \text{ are present} \\ K_d.\ \mathrm{adj} & \text{if } IC_{50} \text{ and } K_d \text{ are present} \\ (K_i.\ \mathrm{adj} + K_d.\ \mathrm{adj})/2 & \text{if } IC_{50},\ K_i, \text{ and } K_d \text{ are present} \end{cases} \quad (5)$$

The KIBA score can be viewed as a model-based summary statistic of all the available information captured by $IC_{50}$, $K_i$, and $K_d$, where the consistency between them is optimized. An assessment of the classification accuracy of the KIBA scoring was based on the expert-classified positive and negative interactions among 365 drug−kinase pairs, for which all three bioactivity types are available from ChEMBL.

## RESULTS AND DISCUSSION

**Overlap and Consistency Across the Three Studies.** As the three comprehensive studies cover the major kinase families with common clinical and experimental compounds, we first evaluated the agreement between the bioactivity types using their shared drug−target interactions. The pairwise overlaps between the three studies were relatively small, indicating that each of the studies focused on profiling specific subsets of kinase inhibitors (Figure 1). However, the number of shared drug−target interactions was large enough to enable comparative analyses, with an average percentage of 14% overlap among the total number of compound−protein interactions profiled (Table 1). Among the pairwise comparisons across the bioactivity types, the Davis $K_d$ and the Metz $K_i$ data showed the highest consistency, with a Kendall rank correlation of 0.5 ($p < 10^{-15}$). When comparing $K_i$ or $K_d$ against the Activity percentage, the correlations started to decrease, with the Kendall correlation being 0.32 and 0.4, respectively (Figure 2),

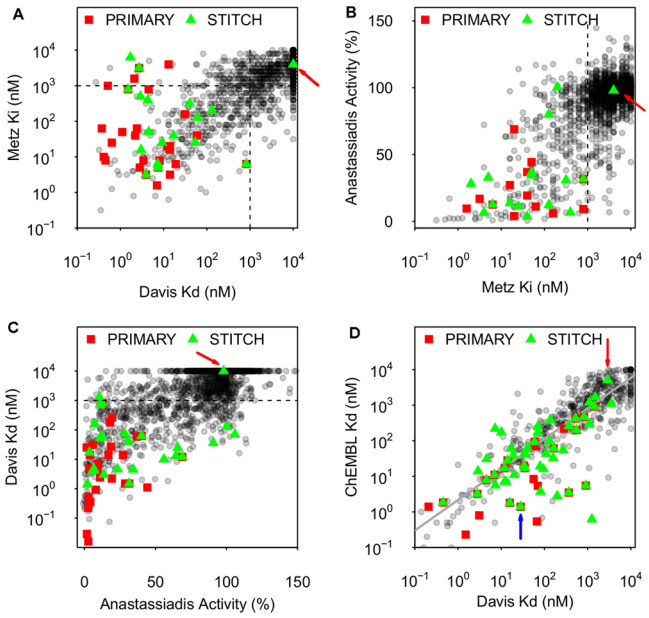


**Figure 2.** (A−C) Pairwise comparison of the bioactivity values across the common drug−target pairs in the three studies. Interactions obtained from the Primary target list (PRIMARY) and the STITCH database (STITCH) are highlighted. Dashed lines: empirical $K_i$ and $K_d$ thresholds for discriminating positive and negative drug−target interactions. Red arrows: imatinib-MAPK14 pair showing consistent high bioactivity values in each assay while being given a high confidence score in STITCH. (D) $K_d$ bioactivity values across the common drug−target pairs between Davis and ChEMBL. Solid line: slope of the linear regression. Dashed line: diagonal. Red arrow: erlotinib-ERBB2 pair. Blue arrow: erlotinib-EGFR pair.

indicating that the Anastassiadis Activity data might not be directly scaled into the inhibition constants. This result was rather expected, since $K_i$ in the Metz study and $K_d$ in the Davis study were derived from biochemical assays tested on a range of concentrations, while the remaining enzyme activity reported in the Anastassiadis data was measured at a single concentration at 0.5 $\mu$M, making it more concentration-specific and less informative for determining drug−target interactions on a quantitative scale.

As shown in Figure 2, the majority of PRIMARY interactions and STITCH interactions can be found both in the Davis and Metz data with bioactivity values smaller than 1000 nM (average $K_d$ = 271 nM and average $K_i$ = 618 nM, respectively). We found that 1000 nM may be considered as an empirical bioactivity threshold for determining true positive interactions with high confidence (sensitivity: 0.85; hypergeometric test, $p < 10^{-15}$). Notably, however, these reported drug−target interactions constitute only a small fraction (10.5%) of the total number of interactions with both $K_i$ and $K_d$ lower than 1000


dx.doi.org/10.1021/ci400709d | J. Chem. Inf. Model. 2014, 54, 735−743

Table 2. Evaluation of ChEMBL and STITCH Databases against the Three Kinase Inhibitor Selectivity Studies[a]

| | | ChEMBL | | | STITCH | | | PRIMARY | | |
|---|---|---|---|---|---|---|---|---|---|---|
| studies | unit | N | KS | Cor | N | ES | NES | N | ES | NES |
| Davis[35] | $K_d$ (nM) | 498 | 0.046 ($p$ = 0.66) | 0.66 ($p$ < 0.001) | 49 | 0.501 | 2.798 ($p$ < 0.001) | 26 | 0.571 | 2.688 ($p$ < 0.001) |
| Metz[36] | $K_i$ (nM) | 41 | 0.390 ($p$ = 0.004) | 0.76 ($p$ < 0.001) | 12 | 0.919 | 1.717 ($p$ = 0.0014) | 3 | 0.868 | 1.292 ($p$ = 0.118) |
| Anastassiadis[37] | Activity (%) | 991 | 0.404 ($p$ < 0.001) | 0.36 ($p$ < 0.001) | 23 | 0.705 | 1.549 ($p$ < 0.001) | 1 | 0.942 | 1.256 ($p$ = 0.130) |

[a]N: number of common compound−protein interactions. KS: Kolmogorov−Smirnov test. Cor: Kendall correlation. ES: enrichment score. NES: normalized enrichment score. STITCH and PRIMARY: drug−target interactions considered in the study.

nM. This clearly indicates that the majority of the potential drug−target interactions discovered by the two studies have not been fully translated into STITCH. Even though the STITCH database is aiming at an integration of multiple data sources, the coverage of the STITCH database on kinase inhibitors, at least for those that have been reported recently, is rather lagging behind. Exploring such new drug−target interaction data provided by these kinome-wide studies therefore is of high importance to identify novel polypharmacological and off-target effects of kinase inhibitors and other potential drug molecules.

Use of the complementary bioactivity profiles from the three studies enables also the projection of the unary drug−target interactions derived from integrated knowledge databases such as STITCH. By identifying notable outliers in the scatterplots, one may start to explore the reliability of such reported positive interactions. For example, according to STITCH, imatinib (ChEMBL ID: ChEMBL941) is interacting with the protein kinase MAPK14 (Uniprot ID: Q16539), with a reasonably high combined confidence score of 938 (Figure 2A−C, indicated by an arrow); however, none of the bioactivity data from the three profiling studies supported such a high confidence interaction ($K_d$ > 10 000 nM, $K_i$ = 3981 nM, and Activity 97.98% at 500 nM). In fact, when exploring in more detail the STITCH database, the high confidence score for the imatinib-MAPK14 pair came solely from two studies where the $IC_{50}$ was reported as 13 700 nM[43] and 100 000 nM,[44] respectively. Given such a high level of $IC_{50}$, the combined confidence score for imatinib-MAPK14 is more likely a curation error in the STITCH database.

**Evaluation of the Data Reproducibility Using ChEMBL.** Since the three profiling studies are utilizing different techniques of competitive assays that result in distinct bioactivity readouts, we next sought to evaluate the reproducibility of the reported values by comparing against other independent studies that were reported in ChEMBL. Duplicated and low-confidence values were removed (see Materials and Methods for details of data extraction and filtering). These filtering steps resulted in 498 drug−target interactions measured in $K_d$, 41 interactions in $K_i$, and 991 interactions in Activity percentage. The drastically decreasing numbers of replicated drug−target interactions are mainly due to the lack of repeated studies in ChEMBL. In fact, many previous studies have considered only a handful of compounds tested against a few targets, making such smaller-scale studies incomparable to the scale of the three studies, which utilized more comprehensive kinome-wide specificity assays that have become available only recently. However, when retrieving the drug−target interactions in common with the Metz data, we found that most of the previous studies are from the same company (Abbott Laboratories), and therefore we excluded them as nonindependent studies (Supporting Information Table 2).

In line with the analysis of the overlap between the three studies, the Davis $K_d$ data showed better consistency with the ChEMBL $K_d$ data in terms of fit in the density distributions (Supporting Information Figure 1). The distributions of the Metz $K_i$ and Anastassiadis Activity, on the other hand, started to differ from the ChEMBL data at the higher affinity levels. Notably, however, the $K_i$ values between the Metz and ChEMBL showed the best agreement in terms of rank-based Kendall correlation (Table 2), indicating that even in the absence of overall distributional similarity, the drug−target interactions are ranked similarly across the different $K_i$ studies. It should be noted, however, that the sample size for evaluating the consistency of the $K_i$ assays is relatively small ($n$ = 41), compared to the data from the $K_d$ assays ($n$ = 498) and the Activity studies ($n$ = 991). The GSEA results also supported the previous observations that the positive interactions from PRIMARY and STITCH lists were, in general, enriched especially in the lower ranges of the $K_d$ spectrum (Table 2), suggesting that $K_d$ provides useful information for discriminating between true positive and negative drug−target interactions.

Mapping of STITCH drug−target interactions onto the quantitative data can also be used for evaluation of their reliability. In particular, those STITCH interactions that are located on the higher end of $K_d$/$K_i$ values might require some attention from the end users, even though they are reported as having high confidence scores by the STITCH algorithm. For example, the binding interaction between erlotinib and ERBB2 (CHEMBL553-P04626) is of very low affinity according to the data from both ChEMBL and the Davis study ($K_d$ = 5100 nM and $K_d$ = 2900 nM, respectively), whereas it was labeled as a high-confidence interaction in STITCH (combined confidence score 954). In fact, according to the Davis data, erlotinib is known to bind specifically to EGFR ($K_d$ = 28 nM) but not ERBB2 (Figure 2D, Supporting Information Figure 2). EGFR and ERBB2 belong to the same ErbB receptor family that also includes ERBB3 and ERBB4. Recent studies have also shown that activation of ERBB2 leads to resistance to EGFR inhibitors.[45] The kinase subfamily link or the physical interaction between ERBB2 and EGFR on the protein level seems to be the reason behind the erroneous high confidence score for the erlotinib-ERBB2 pair in STITCH (Figure 3).

**Integration of Kinase Inhibitor Bioactivity Data.** A practical challenge when using ChEMBL or other compound bioactivity databases is that there exist multiple replications that differ between studies for a given drug−target pair. The number of bioactivity types deposited in ChEMBL is high (over 600 altogether), but their distribution is highly skewed toward a few major types. $IC_{50}$, $K_i$, and $K_d$ values are among the most abundant ones (Supporting Information Figure 3), and these bioactivity types also showed relatively high consistency (Table 3). We note that other biochemical assays including Inhibition, Potency, and Activity, are also widely reported in ChEMBL, but


dx.doi.org/10.1021/ci400709d | J. Chem. Inf. Model. 2014, 54, 735−743

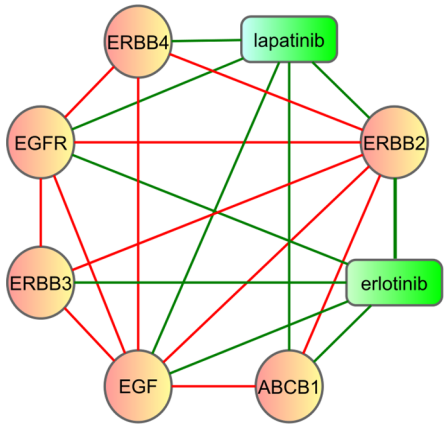


**Figure 3.** The STITCH chemical-protein interaction networks for erlotinib and lapatinib. Protein−protein interactions are shown in red, while chemical−protein interactions are in green. Erlotinib has been found erroneously linked to ERBB2, ERRB3, and EGF in STITCH.

**Table 3. Integrated KIBA Score Compared with $IC_{50}$, $K_i$, and $K_d$ Bioactivity Types[a]**

| | $IC_{50}$ | $K_i$ | $K_d$ | KIBA |
|---|---|---|---|---|
| $IC_{50}$ | | 0.72 | 0.63 | 0.77 |
| $K_i$ | 0.67 | | 0.50 | 0.76 |
| $K_d$ | 0.78 | | | 0.73 |
| KIBA | 0.71 | 0.29 | 0.38 | |

[a]Upper-diagonal: Kendall rank correlation. Lower-diagonal: Jaccard distance.

their overlap with $IC_{50}$ and $K_i$ was surprisingly low, and their values do not correlate well (Supporting Information Figure 4). There is a lack of consistency also between the Inhibition and Activity, which is likely due to the ambiguous definitions of these bioactivity types in different studies. For example, by definition, Activity should refer to the remaining enzyme activity, but we found that many values reported in ChEMBL stand for the percentage of inhibited activity, which is the opposite. Pooling all the activity values without differentiating the apparently contradictory interpretations will lead to a bimodal distribution (Supporting Information Figure 4), in which the majority of values are centered either at 0% or 100%, both of which should be interpreted as negative interactions. Therefore, to avoid such hidden confounding factors, we focused in the following on the three standardized bioactivity types, including $IC_{50}$, $K_i$, and $K_d$, to derive the integrated bioactivity scores for kinase inhibitors.

A total of 246 088 drug−kinase interactions, including 52 498 drugs and 467 kinases, were found from ChEMBL that reported $IC_{50}$, $K_i$, or $K_d$ values. The median after log 10 transformation was taken if there were multiple measurements of the same measurement type. It was observed that $IC_{50}$ and $K_i$ values were more consistent with each other than when compared with $K_d$ values, which can be seen from both their higher Kendall rank correlations and their lower pairwise Jaccard distances (Table 3). This was expected since $IC_{50}$ and $K_i$ readouts are directly related through the Cheng-Prusoff model in a typical enzymatic inhibition assay. The $K_d$ values, on the other hand, are less correlated as the binding mechanisms with the ATP sites are more compound-dependent (Table 3). After determining empirically the parameters $L_i = 0.3$ and $L_d = 1.3$ in eq 4, it was found that the model-based adjustment further improved the pairwise correlations between the $K_i$ and $K_d$ bioactivity types (Figure 4, Supporting Information Figure 5). Moreover, the integrated bioactivity KIBA scores, as calculated using eq 5, further improved the mutual consistency among all three bioactivity types (Table 3). These results indicate that KIBA can conceptually be considered as the geometric center of the three bioactivity types, from where the pairwise distances are optimized (Figure 5).

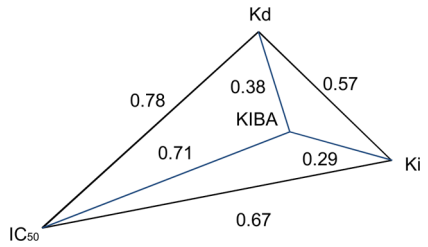


**Figure 5.** A schematic illustration of how the KIBA integration improves the consistency between the three bioactivity types ($IC_{50}$, $K_i$, and $K_d$). The Jaccard distances are shown on the connecting edges.

To investigate the potential advantages of using the integrated KIBA scores, we compiled 365 drug−kinase pairs for which $IC_{50}$, $K_i$, and $K_d$ bioactivity types are available in ChEMBL. The positive and negative interactions among these drug−kinase pairs were manually curated using expert knowledge, and these served as the ground truth for the classification accuracy (Supporting Information data). We found that the

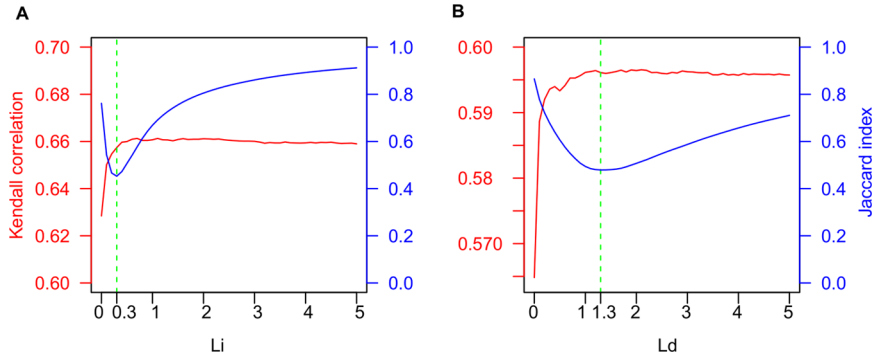


**Figure 4.** Optimization of the parameters $L_i$ and $L_d$ in the KIBA integration model improves the consistency between $K_i$ and $K_d$ levels The optimal adjustment for $K_i$ was found at $L_i = 0.3$ (A, green dashed line) and $K_d$ at $L_d = 1.3$ (B, green dashed line). In both cases, the Jaccard distance was minimized at the point where the Kendall correlation starts to stabilize.


dx.doi.org/10.1021/ci400709d | J. Chem. Inf. Model. 2014, 54, 735−743

KIBA values gave the highest AUC, indicating its enhanced power to discriminate between true positive and negative drug−target interactions, compared to using $IC_{50}$, $K_i$, or $K_d$ alone ($p$ = 0.021, 0.0001, and 0.037; De Long's test, Figure 6A).

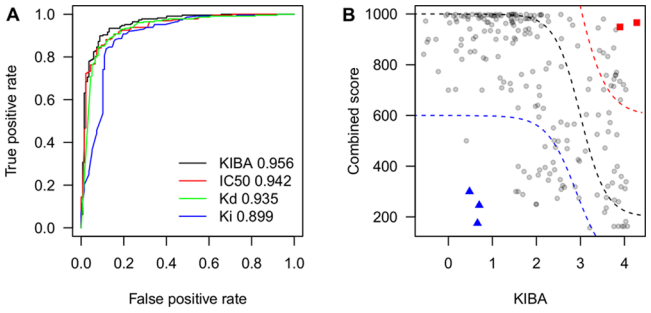


**Figure 6.** Prediction of true positive and negative drug−target interactions using the integrated KIBA bioactivity scores. (A) The predictive accuracy of KIBA as compared to those using the individual bioactivity types alone. The areas under the ROC curves (AUC) are shown in the legend. (B) Correlation between the KIBA and the combined score in STITCH. Four-parameter logistic functions were used for curve fitting. Black dashed line: slope = 1.5, min = 200, max = 1000, inflection = 1000. Red dashed lines: slope = 1.3, min = 0, max = 600, inflection = 800. Blue dashed lines: slope = 1.3, min = 600, max = 1600, inflection = 800. The parameters for the upper and lower bounds were chosen to reflect the empirical KIBA threshold (1000 nM) for classifying drug−target interactions. Red squares: imatinib-EGFR and imatinib-SRC. Blue triangles: dasatinib-PTK6, staurosporine-CDK9, and vemurafenib-RAF1.

Even if KIBA has a smaller difference in AUC with $IC_{50}$ than $K_d$, the difference is more significant due to a higher covariance. More specifically, KIBA showed systematically the best sensitivity of interaction detections, except for the highest specificity levels, where $IC_{50}$ was performing equally well, while its accuracy decreased after moving beyond the most obvious drug−target interactions. Surprisingly, $K_i$ values showed relatively low prediction power, perhaps due to the fact that most of the $K_i$ data for these 365 drug−target pairs were extracted from the Metz data (319 values out of 468 including multiple values for the same drug−target pair). A lack of sufficient variation in the data sources for the $K_i$ type may make it relatively underpowered to detect the true drug−target interactions.

The integrated KIBA score enabled us also to construct a quantitative bioactivity matrix among kinase inhibitors and their potential targets (Supporting Information data), which can further provide guidelines on classifying positive and negative interactions. We note that the KIBA method is applicable also to cases where only two out of the three bioactivity types are available, where the KIBA score can be predicted using eq 5. Along the same lines, KIBA scores can be used to impute those drug−target pairs that are missing in the databases, such as STITCH, or even point out potential erroneous interactions. For instance, if a drug−target pair with a high STITCH score is found to have a high KIBA score, the interaction may warrant further curation (Figure 6B). We have compiled accordingly a table that includes a set of likely incorrectly scored drug−target interactions in STITCH (Supporting Information data). As an example, we pinpointed three drug−target interactions (dasatinib-PTK6, staurosporine-CDK9, and vemurafenib-RAF1), which might be associated with too low combined scores in STITCH. Interestingly, we also found two potential false positive imatinib-related interactions (imatinib-EGFR and imatinib-SRC), which lack experimental biochemical evidence for their high combined scores in STITCH. Although imatinib has been shown to bind to the kinase domain of SRC in a crystal structure,[46] it has a very low affinity to the SRC kinase according to all binding and bioactivity data we have collected (Supporting Information Table 4). Therefore, we consider this interaction highly unlikely to be physiologically relevant.

## CONCLUSIONS

By means of a systematic evaluation of the kinase bioactivity data, obtained from three large-scale profiling studies as well as from ChEMBL and STITCH databases, we found out that the $K_d$ binding affinity assays provided a reproducible source of drug−target interactions. Most of the currently reported $K_d$ data for kinase inhibitors are based on the Ambit/KINOMEscan platform, which might partly explain such a high consistency. It is therefore likely that experimental differences, for instance, in ATP concentrations, protein/peptide phosphate donor substrates, kinase domain fragments, or their phosphorylation states contributed to the observed differences in the $K_i$, $IC_{50}$, and Activity results. When extended to the ChEMBL-level investigation, the consistency between $IC_{50}$, $K_i$, and $K_d$ could be significantly improved through using the model-based adjustments. While the number of overlapping drug−target interactions is currently too limited to make any definite conclusions, the ChEMBL database is constantly increasing in the coverage of kinase inhibitor assays, and therefore it is expected that the evaluation of other bioactivity types than $K_d$ will become more accurate in the future. It was also observed that the Activity readout does not provide in its current form highly reproducible drug−target interaction data. A straightforward solution would be to report in ChEMBL also the compound concentration levels and ranges to estimate the dose−response curve, so that Activity could be directly related to other bioactivities such as $IC_{50}$, $K_i$, and $K_d$.

While most of the drug−target interactions reported in STITCH present with sufficiently low bioactivity values, indicating true interactions, there are also a number of obvious false positive interactions that need some attention from the end users when making use of the interactions reported in STITCH. In the current version of STITCH, the drug−target interactions are limited to positive cases only, with confidence scores combining evidence from multiple sources. Importantly, a missing drug−target interaction in STITCH does not necessarily indicate its absence, unless there are experimental data found from the literature to support such noninteraction. Databases such as STITCH should ideally report also the true negative cases that include drug−target interactions that were tested but for which interaction was not detected. Furthermore, drug−target interactions in STITCH are accessible for single compounds only, while cross-talks between the compounds are largely missing from such a compound-centric view. Ideally, drug−drug interaction networks could be built by linking the targets via the reported protein−protein interactions, as shown in Figure 3. Such networks that map interactions between multiple compounds and their protein targets might have the potential to facilitate polypharmacology design for many applications, such as those geared toward phenotype-based drug discovery or drug repurposing.[47]

In addition to the comparative evaluations across the bioactivity types, we also introduced a novel bioactivity score, which integrates complementary information from the three


dx.doi.org/10.1021/ci400709d | J. Chem. Inf. Model. 2014, 54, 735−743

major bioactivity types ($IC_{50}$, $K_i$, and $K_d$). The integrated KIBA score was shown to maximize their mutual consistency. Furthermore, the integration of bioactivity measurements through the model-based fitting facilitated the detection of true drug−target interactions across the whole specificity spectrum. Even though the difference between KIBA and $K_d$ was not significant in this limited set of kinase inhibitors and their target, KIBA demonstrated its potential to make use of the information captured by the various inhibitory measurements, which should prove useful in broader families of compounds and their target spaces. Also, the improved correlation observed among the $K_i$ and $K_d$ after the model-based adjustment indicates that any missing or unreliable bioactivity measurements in individual studies might be predicted from the other measurements at a reasonable accuracy. As one example of how to make use of such an integrated bioactivity scoring, we pinpointed interactions reported in STITCH for further manual curation. The future integrated analysis could be improved further if ChEMBL and other databases provided more experimental details associated with the extracted bioactivity values, including their dose ranges and $K_m/[S]$ ratios.

We have also made publicly available the integrated drug−target bioactivity data, which contains the bioactivity measurements evaluated in the present study, as well as their integrated KIBA scores, to promote their usage both in drug discovery developments and as a bench-marking data set for testing computational approaches to drug−target interaction prediction. The procedures developed and applied here can also be utilized as more generic guidelines on how to compare and integrate the bioactivity data from current and emerging studies. Comprehensive profiling studies of kinase inhibitor specificity have only recently started to appear in publications, and their systematic comparison should lead to better understanding of the strengths and limitations of the different assay formats.[48] Large-scale studies that utilize either the same or complementary assay types and readouts, such as thermal stability shift assays,[49] could be incorporated in the evaluation framework in the future extensions. As an example, a recent study[50] used the fold-change of decreased HSP90 chaperone for the ATP-competitive substrate as a drug−target interaction readout. Including such a fold-change bioactivity type should provide additional insights into the kinase inhibitor specificities and their cell-based activities. However, since its overlap with the selected three studies is quite limited (Supporting Information Figure 6), we decided not to include this study in the current comparative analysis.

## ■ ASSOCIATED CONTENT

### Supporting Information

Figures S1−S6 and Tables S1−S4 show additional results. Data file in Excel format reports the bioactivity values for the overlapping drug−target pairs between the three studies and the KIBA scores that are derived through mining the ChEMBL database. This material is available free of charge via the Internet at http://pubs.acs.org.

## ■ AUTHOR INFORMATION


### Corresponding Author

*E-mail: jing.tang@fimm.fi.


### Author Contributions

Conceived and designed the study: J.T., P.H., K.W., and T.A. Performed the analysis: J.T., P.H., T.X., S.S., A.S. Wrote the paper: J.T., K.W., T.A. The manuscript was written through contributions of all authors. All authors have given approval to the final version of the manuscript.


### Funding

This work was funded by the Academy of Finland (No. 120569, 133227, 140880, 269862 and 272437), the Jane and Aatos Erkko Foundation, the Centre for International Mobility (CIMO), and the Helsinki Biomedical Graduate Program (HBGP).


### Notes

The authors declare no competing financial interest.

## ■ ACKNOWLEDGMENTS


We thank the authors of the Davis et al., Metz et al., and Anastassiadis et al. studies for making their bioactivity data publicly available, as well as the ChEMBL team for giving us the permission to redistribute the bioactivity data analyzed in the present study.


## ■ ABBREVIATIONS

GSEA, gene set enrichment analysis; ES, enrichment scores; NES, normalized enrichment scores; AUC, area under the receiver operating characteristic curve

## ■ REFERENCES


(1) Overington, J. P.; Al-Lazikani, B.; Hopkins, A. L. How many drug targets are there? *Nat. Rev. Drug Discovery* **2006**, *5*, 993−996.

(2) Hopkins, A. L. Network pharmacology: the next paradigm in drug discovery. *Nat. Chem. Biol.* **2008**, *4*, 682−690.

(3) Tang, J.; Karhinen, L.; Xu, T.; Szwajda, A.; Yadav, B.; Wennerberg, K.; Aittokallio, T. Target inhibition networks: predicting selective combinations of druggable targets to block cancer survival pathways. *PLoS Comput. Biol.* **2013**, *9*, e1003226.

(4) Xie, L.; Xie, L.; Kinnings, S. L.; Bourne, P. E. Novel computational approaches to polypharmacology as a means to define responses to individual drugs. *Annu. Rev. Pharmacol. Toxicol.* **2012**, *52*, 361−379.

(5) Kitano, H. A robustness-based approach to systems-oriented drug design. *Nat. Rev. Drug Discovery* **2007**, *6*, 202−210.

(6) Lehár, J.; Krueger, A. S.; Avery, W.; Heilbut, A. M.; Johansen, L. M.; Price, E. R.; Rickles, R. J.; Short, G. F., 3rd; Staunton, J. E.; Jin, X.; Lee, M. S.; Zimmermann, G. R.; Borisy, A. A. Synergistic drug combinations tend to improve therapeutically relevant selectivity. *Nat. Biotechnol.* **2009**, *27*, 659−666.

(7) Knight, Z. A.; Lin, H.; Shokat, K. M. Targeting the cancer kinome through polypharmacology. *Nat. Rev. Cancer* **2010**, *10*, 130−137.

(8) Karczewski, K. J.; Daneshjou, R.; Altman, R. B. Chapter 7: Pharmacogenomics. *PLoS Comput. Biol.* **2012**, *8*, e1002817.

(9) Futamura, Y.; Muroi, M.; Osada, H. Target identification of small molecules based on chemical biology approaches. *Mol. Biosyst.* **2013**, *9*, 897−914.

(10) Zhao, S.; Iyengar, R. Systems pharmacology: network analysis to identify multiscale mechanisms of drug action. *Annu. Rev. Pharmacol. Toxicol.* **2012**, *52*, 505−521.

(11) Tang, J.; Aittokallio, T. Network pharmacology strategies toward multi-target anticancer therapies: from computational models to experimental design principles. *Curr. Pharm. Des.* **2014**, *20*, 23−36.

(12) Li, Y. Y.; Jones, S. J. Drug repositioning for personalized medicine. *Genome Med.* **2012**, *4*, 27.

(13) Yildirim, M. A.; Goh, K.-I.; Cusick, M. E.; Barabási, A.-L.; Vidal, M. Drug-target network. *Nat. Biotechnol.* **2007**, *25*, 1119−1126.

(14) Janga, S. C.; Tzakos, A. Structure and organization of drug−target networks: insights from genomic approaches for drug discovery. *Mol. Biosyst.* **2009**, *5*, 1536−1548.
(15) Azuaje, F. J.; Zhang, L.; Devaux, Y.; Wagner, D. R. Drug-target network in myocardial infarction reveals multiple side effects of unrelated drugs. *Sci. Rep.* **2011**, *1*, 52.
(16) Takigawa, I.; Tsuda, K.; Mamitsuka, H. Mining significant substructure pairs for interpreting polypharmacology in drug−target network. *PloS One* **2011**, *6*, e16999.
(17) Cheng, F.; Liu, C.; Jiang, J.; Lu, W.; Li, W.; Liu, G.; Zhou, W.; Huang, J.; Tang, Y. Prediction of drug−target interactions and drug repositioning via network-based inference. *PLoS Comput. Biol.* **2012**, *8*, e1002503.
(18) Mestres, J.; Gregori-Puigjané, E.; Valverde, S.; Solé, R. V. Data completeness–the Achilles heel of drug−target networks. *Nat. Biotechnol.* **2008**, *26*, 983−984.
(19) Kanehisa, M.; Goto, S.; Sato, Y.; Furumichi, M.; Tanabe, M. KEGG for integration and interpretation of large-scale molecular data sets. *Nucleic Acids Res.* **2012**, *40*, D109−114.
(20) Chang, A.; Scheer, M.; Grote, A.; Schomburg, I.; Schomburg, D. *Nucleic Acids Res.* **2009**, *37*, D588−592.
(21) Hecker, N.; Ahmed, J.; von Eichborn, J.; Dunkel, M.; Macha, K.; Eckert, A.; Gilson, M. K.; Bourne, P. E.; Preissner, R. SuperTarget goes quantitative: update on drug−target interactions. *Nucleic Acids Res.* **2012**, *40*, D1113−1117.
(22) Zhu, F.; Shi, Z.; Qin, C.; Tao, L.; Liu, X.; Xu, F.; Zhang, L.; Song, Y.; Liu, X.; Zhang, J.; Han, B.; Zhang, P.; Chen, Y. Therapeutic target database update 2012: a resource for facilitating target-oriented drug discovery. *Nucleic Acids Res.* **2012**, *40*, D1128−1136.
(23) Knox, C.; Law, V.; Jewison, T.; Liu, P.; Ly, S.; Frolkis, A.; Pon, A.; Banco, K.; Mak, C.; Neveu, V.; Djoumbou, Y.; Eisner, R.; Guo, A. C.; Wishart, D. S. DrugBank 3.0: a comprehensive resource for 'omics' research on drugs. *Nucleic Acids Res.* **2011**, *39*, D1035−1041.
(24) Yamanishi, Y. Chemogenomic approaches to infer drug−target interaction networks. *Methods Mol. Biol.* **2013**, *939*, 97−113.
(25) Gönen, M. Predicting drug−target interactions from chemical and genomic kernels using Bayesian matrix factorization. *Bioinformatics* **2012**, *28*, 2304−2310.
(26) Chen, H.; Zhang, Z. A semi-supervised method for drug−target interaction prediction with consistency in networks. *PloS One* **2013**, *8*, e62975.
(27) Pahikkala, T.,; Airola, A.; Pietilä, S.; Shakyawar, S.; Szwajda, A.; Tang, J.; Aittokallio, T. Toward more realistic drug−target interaction predictions. Submitted.
(28) Gaulton, A.; Bellis, L. J.; Bento, A. P.; Chambers, J.; Davies, M.; Hersey, A.; Light, Y.; McGlinchey, S.; Michalovich, D.; Al-Lazikani, B.; Overington, J. P. ChEMBL: a large-scale bioactivity database for drug discovery. *Nucleic Acids Res.* **2012**, *40*, D1100−1107.
(29) Lounkine, E.; Keiser, M. J.; Whitebread, S.; Mikhailov, D.; Hamon, J.; Jenkins, J. L.; Lavan, P.; Weber, E.; Doak, A. K.; Côté, S.; Shoichet, B. K.; Urban, L. Large-scale prediction and testing of drug activity on side-effect targets. *Nature* **2012**, *486*, 361−367.
(30) Gfeller, D.; Michielin, O.; Zoete, V. Shaping the interaction landscape of bioactive molecules. *Bioinformatics* **2013**, *29*, 3073−3079.
(31) Martínez-Jiménez, F.; Papadatos, G.; Yang, L.; Wallace, I. M.; Kumar, V.; Pieper, U.; Sali, A.; Brown, J. R.; Overington, J. P.; Marti-Renom, M. A. Target prediction for an open access set of compounds active against mycobacterium tuberculosis. *PLoS Comput. Biol.* **2013**, *9*, e1003253.
(32) Kruger, F. A.; Overington, J. P. Global analysis of small molecule binding to related protein targets. *PLoS Comput. Biol.* **2012**, *8*, e1002333.
(33) Kramer, C.; Kalliokoski, T.; Gedeck, P.; Vulpetti, A. The experimental uncertainty of heterogeneous public K(i) data. *J. Med. Chem.* **2012**, *55*, 5165−5173.
(34) Kalliokoski, T.; Kramer, C.; Vulpetti, A.; Gedeck, P. Comparability of mixed $IC_{50}$ data - a statistical analysis. *PloS One* **2013**, *8*, e61007.
(35) Davis, M. I.; Hunt, J. P.; Herrgard, S.; Ciceri, P.; Wodicka, L. M.; Pallares, G.; Hocker, M.; Treiber, D. K.; Zarrinkar, P. P. Comprehensive analysis of kinase inhibitor selectivity. *Nat. Biotechnol.* **2011**, *29*, 1046−1051.
(36) Metz, J. T.; Johnson, E. F.; Soni, N. B.; Merta, P. J.; Kifle, L.; Hajduk, P. J. Navigating the kinome. *Nat. Chem. Biol.* **2011**, *7*, 200−202.
(37) Anastassiadis, T.; Deacon, S. W.; Devarajan, K.; Ma, H.; Peterson, J. R. Comprehensive assay of kinase catalytic activity reveals features of kinase inhibitor selectivity. *Nat. Biotechnol.* **2011**, *29*, 1039−1045.
(38) Kuhn, M.; Szklarczyk, D.; Franceschini, A.; von Mering, C.; Jensen, L. J.; Bork, P. STITCH 3: zooming in on protein-chemical interactions. *Nucleic Acids Res.* **2012**, *40*, D876−880.
(39) Karaman, M. W.; Herrgard, S.; Treiber, D. K.; Gallant, P.; Atteridge, C. E.; Campbell, B. T.; Chan, K. W.; Ciceri, P.; Davis, M. I.; Edeen, P. T.; Faraoni, R.; Floyd, M.; Hunt, J. P.; Lockhart, D. J.; Milanov, Z. V.; Morrison, M. J.; Pallares, G.; Patel, H. K.; Pritchard, S.; Wodicka, L. M.; Zarrinkar, P. P. A quantitative analysis of kinase inhibitor selectivity. *Nat. Biotechnol.* **2008**, *26*, 127−132.
(40) Subramanian, A.; Tamayo, P.; Mootha, V. K.; Mukherjee, S.; Ebert, B. L.; Gillette, M. A.; Paulovich, A.; Pomeroy, S. L.; Golub, T. R.; Lander, E. S.; Mesirov, J. P. Gene set enrichment analysis: a knowledge-based approach for interpreting genome-wide expression profiles. *Proc. Natl. Acad. Sci. U.S.A.* **2005**, *102*, 15545−15550.
(41) Robin, X.; Turck, N.; Hainard, A.; Tiberti, N.; Lisacek, F.; Sanchez, J.-C.; Müller, M. pROC: an open-source package for R and S + to analyze and compare ROC curves. *BMC Bioinf.* **2011**, *12*, 77.
(42) Cer, R. Z.; Mudunuri, U.; Stephens, R.; Lebeda, F. J. IC50-to-Ki: a web-based tool for converting IC50 to Ki values for inhibitors of enzyme activity and ligand binding. *Nucleic Acids Res.* **2009**, *37*, W441−445.
(43) Chen, N.; Bürli, R. W.; Neira, S.; Hungate, R.; Zhang, D.; Yu, V.; Nguyen, Y.; Tudor, Y.; Plant, M.; Flynn, S.; Meagher, K. L.; Lee, M. R.; Zhang, X.; Itano, A.; Schrag, M.; Xu, Y.; Ng, G. Y.; Hu, E. Discovery of a potent and selective c-Kit inhibitor for the treatment of inflammatory diseases. *Bioorg. Med. Chem. Lett.* **2008**, *18*, 4137−4141.
(44) Dietrich, J.; Hulme, C.; Hurley, L. H. The design, synthesis, and evaluation of 8 hybrid DFG-out allosteric kinase inhibitors: a structural analysis of the binding interactions of Gleevec, Nexavar, and BIRB-796. *Bioorg. Med. Chem.* **2010**, *18*, 5738−5748.
(45) Yonesaka, K.; Zejnullahu, K.; Okamoto, I.; Satoh, T.; Cappuzzo, F.; Souglakos, J.; Ercan, D.; Rogers, A.; Roncalli, M.; Takeda, M.; Fujisaka, Y.; Philips, J.; Shimizu, T.; Maenishi, O.; Cho, Y.; Sun, J.; Destro, A.; Taira, K.; Takeda, K.; Okabe, T.; Swanson, J.; Itoh, H.; Takada, M.; Lifshits, E.; Okuno, K.; Engelman, J. A.; Shivdasani, R. A.; Nishio, K.; Fukuoka, M.; Varella-Garcia, M.; Nakagawa, K.; Jänne, P. A. Activation of ERBB2 signaling causes resistance to the EGFR-directed therapeutic antibody cetuximab. *Sci. Transl. Med.* **2011**, *3*, 99ra86.
(46) Seeliger, M. A.; Nagar, B.; Frank, F.; Cao, X.; Henderson, M. N.; Kuriyan, J. c-Src binds to the cancer drug imatinib with an inactive Abl/c-Kit conformation and a distributed thermodynamic penalty. *Structure* **2007**, *15*, 299−311.
(47) Iorio, F.; Rittman, T.; Ge, H.; Menden, M.; Saez-Rodriguez, J. Transcriptional data: a new gateway to drug repositioning? *Drug Discovery Today* **2013**, *18*, 350−357.
(48) Zhang, C.; Habets, G.; Bollag, G. Interrogating the kinome. *Nat. Biotechnol.* **2011**, *29*, 981−983.
(49) Fedorov, O.; Marsden, B.; Pogacic, V.; Rellos, P.; Müller, S.; Bullock, A. N.; Schwaller, J.; Sundström, M.; Knapp, S. A systematic interaction map of validated kinase inhibitors with Ser/Thr kinases. *Proc. Natl. Acad. Sci. U. S. A.* **2007**, *104*, 20523−20528.
(50) Taipale, M.; Krykbaeva, I.; Whitesell, L.; Santagata, S.; Zhang, J.; Liu, Q.; Gray, N. S.; Lindquist, S. Chaperones as thermodynamic sensors of drug−target interactions reveal kinase inhibitor specificities in living cells. *Nat. Biotechnol.* **2013**, *31*, 630−637.